

Article

# A Meso-Mechanical Constitutive Model of Particle-Reinforced Titanium Matrix Composites at High Temperatures

Weidong Song<sup>1,\*</sup>, Liansong Dai<sup>1</sup>, Lijun Xiao<sup>1</sup>, Cheng Wang<sup>1</sup>, Xiaonan Mao<sup>2</sup> and Huiping Tang<sup>2</sup>

<sup>1</sup> School of Mechatronical Engineering, Beijing Institute of Technology, Beijing 100081, China; dailiansong@yahoo.com (L.D.); xiaolijun20081016@gmail.com (L.X.); wangcheng@bit.edu.cn (C.W.)

<sup>2</sup> Northwest Institute for Non-ferrous Metal Research, Xi'an 710016, China; maonx2014@163.com (X.M.); hptang@c-nin.com (H.T.)

\* Correspondence: swdgh@bit.edu.cn; Tel.: +86-10-6891-4152

Academic Editor: Manoj Gupta

Received: 31 October 2016; Accepted: 26 December 2016; Published: 7 January 2017

**Abstract:** The elastoplastic properties of TiC particle-reinforced titanium matrix composites (TiC/TMCs) at high temperatures were examined by quasi-static tensile experiments. The specimens were stretched at 300 °C, 560 °C, and 650 °C, respectively at a strain rate of 0.001/s. scanning electron microscope (SEM) observation was carried out to reveal the microstructure of each specimen tested at different temperatures. The mechanical behavior of TiC/TMCs was analyzed by considering interfacial debonding afterwards. Based on Eshelby's equivalent inclusion theory and Mori-Tanaka's concept of average stress in the matrix, the stress or strain of the matrix, the particles, and the effective stiffness tensor of the composite were derived under prescribed traction boundary conditions at high temperatures. The plastic strains due to the thermal mismatch between the matrix and the reinforced particles were considered as eigenstrains. The interfacial debonding was calculated by the tensile strength of the particles and debonding probability was described by Weibull distribution. Finally, a meso-mechanical constitutive model was presented to explore the high-temperature elastoplastic properties of the spherical particle-reinforced titanium matrix composites by using a secant modulus method for the interfacial debonding.

**Keywords:** titanium matrix composite; constitutive model; interfacial debonding; high temperature; elastoplastic properties

## 1. Introduction

Titanium matrix composites (TMCs) become ideal materials for auto industry [1] and shipbuilding industry [2,3], with high specific strength, high specific modulus, and high temperature resistance. TMCs are mainly divided into two categories, continuously reinforced titanium matrix composites and particle-reinforced titanium matrix composites. Among them, particle-reinforced TMCs develop rapidly due to isotropic characteristics, high temperature properties, as well as low cost compared to the continuously-reinforced TMCs [4]. In order to achieve excellent properties, it is essential for reinforced particulates to have superior mechanical properties and also combine stably with the matrix materials [5]. Several ceramic particles were proposed as titanium reinforcements: SiC, B<sub>4</sub>C, TiAl, TiB<sub>2</sub>, TiN, TiC, and TiB [5–8]. Particularly, TiC was an excellent choice for its high modulus, strength, stiffness, hardness, and compatibility with titanium matrix [9,10]. According to the literature, TiC/Ti bulk nanocomposites have been significantly studied by Gu et al. [11,12], which systematically presented the influence of TiC on Ti matrix phase, densification, microstructure, and strengthening mechanisms.

A series of theory about particulate-reinforced composites taking account of particle size effects, damage evolution and debonding damage was carried out by K. Tohgo [13–16]. The coupled effects of the temperature and strain rate were studied by Song et al. [17,18], and a modified Johnson–Cook model was proposed to predict the dynamic behavior of TiCp/Ti. Recently, the combination of macroscopic and mesoscopic methods have been widely used to investigate dynamic mechanical behaviors and constitutive model. Meso-mechanical damage theory considers the variation of stiffness/compliance tensor as one measure of the damage, so how to determine the effective elastic modulus of the damaged materials becomes a key problem.

Main meso-mechanical theories are outlined as follows: Eshelby's equivalent inclusion theory [19,20], self-consistent theory [21,22], Mori-Tanaka's theory [23], differential schemes [24], Hashin-Shtrikman Bounds [25,26], and so on. The elastoplastic behavior of the particle-reinforced composite with damage is widely explored by using the first-order stress moment, second-order stress moment, secant modulus method, and incremental method [27–29], the damage patterns include crack or hole in the matrix, interfacial debonding, particle fracture, and so on. In our previous work [30], a one-dimension dynamic constitutive model based on Eshelby's equivalent inclusion theory and Mori-Tanaka theory was established, by adding micro-crack nucleation and growth model. A three-dimensional interfacial debonding model to predict the stress-strain responses of weakly bonded composites was proposed by Lissenden [31], which was based on a modified Needleman type cohesive zone model. Considering progressively weakened interface, an elasto-plastic multi-level damage model was developed to predict the effective elasto-plastic behavior of particle-reinforced metal matrix composites in the work of Lee and Pyo [32]. According to Xia and Wang [33], a micromechanical model based on the analysis of localized deformation bands was provided to predict the toughening of dual-phase composites. However, there is little literature on the elastoplastic behavior of particle-reinforced composite at high temperatures. Whether the models widely used at room temperature still effective at high temperatures in new materials still have not identified by research.

In the current paper, the elastoplastic behavior of TiC particle-reinforced composite with interfacial debonding at high temperatures is discussed by means of Mori-Tanaka's mean field theory in conjunction with Eshelby's equivalent inclusion theory. A meso-mechanical constitutive model is proposed to predict the mechanical properties of the composite at high temperatures by considering the interfacial debonding.

## 2. Experimental Procedure

### 2.1. Materials

The material of titanium matrix composite reinforced with 3% TiCp was provided by Northwest Institute for Nonferrous Metal Research, which was manufactured by the pre-treatment melt process. The composition of the titanium matrix alloy was Ti-6Al-2.5Sn-4Zr-0.5Mo-1Nb-0.45Si, which could be used at high temperature ranging from 600 °C to 620 °C with excellent strength and oxidation resistance maintained above 600 °C. The reinforced particle dispersed homogeneously in the matrix which had an average diameter of about 5 μm [34] and no brittle phase existed. The interfacial reaction layers between the particle and the matrix were stable and the reaction zone width was below 3 μm, by which perfect ductility at room temperature and strength ratio above 650 °C were demonstrated.

### 2.2. Specimen Preparation

Specimens for quasi-static tensile tests were machined by linear cutting, which were in a shape of flat dumbbell with holes at both ends to be clamped. The thickness was 3 mm and the schematic of the specimens was presented in Figure 1.

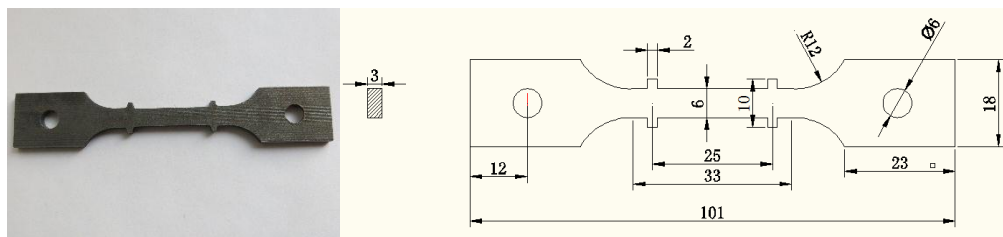


**Figure 1.** Specimen for quasi-static tensile test (unit: mm).

### 2.3. Quasi-Static Tensile Tests

The quasi-static tensile tests at elevated temperatures were carried on WDW-300 electronic universal testing machine (Jinan East Testing Machine Co., Ltd., Jinan, China). The temperature and measurement were controlled by GW-1200A controller and high-temperature furnace, respectively, during testing. The tests was conducted at deformation temperatures of 300 °C, 560 °C, and 650 °C with the same strain rate of  $10^{-3} \text{ s}^{-1}$ . The heat should be preserved for 5–10 min to ensure a uniform temperature in the test piece after the specimens were heated to the experimental temperature. Each experimental condition was repeated at least three times, and the average was taken from two valid experimental data of good reproducibility to be the final result. SEM tests were performed by a BCPCAS4800 scanning electron microscope (JEOL Co., Ltd., Tokyo, Japan) to observe the fracture morphology of each specimen stretched at different temperatures.

### 2.4. Experimental Results

#### 2.4.1. Microstructure

The images in Figure 2 exhibit the fracture microstructure of TiC/TMCs composites samples tested at different temperatures. The results reveal that the failure of the composites is dominant by the interface debonding, particle cracking, and ductile fracture of the matrix. It can be seen that with the temperature rises up, the dimples of fracture surface tend to be more uniformly distributed. The sizes of dimples are getting to be larger and deeper when the experimental temperature increases from 300 °C to 650 °C. This demonstrates that the TiC/TMCs composites show better plasticity at elevated temperature.

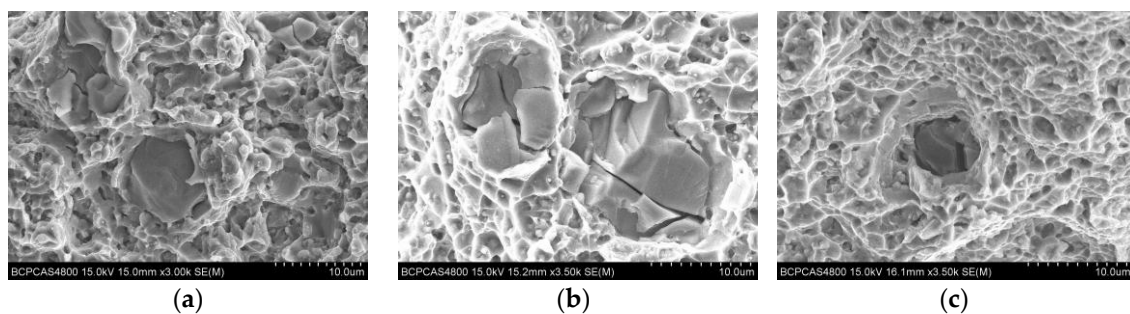


**Figure 2.** SEM images of TiC/TMCs composites: (a) 300 °C; (b) 560 °C; and (c) 650 °C.

#### 2.4.2. Stress-Strain Relationship

Figure 3 shows the results of the quasi-static stress-strain curves for the titanium matrix composite at different temperatures. According to the tests, it is obvious that the TiC/TMCs composites demonstrate temperature sensitivity. The flow stress decreases with increasing experimental temperature at the same strain rate. From the data at 300 °C and 560 °C, the typical strain hardening curve can be obtained, but the flow stress of the latter rises more slowly than the former. For the

stress-strain curve at 650 °C, the flow stress dropped with increasing strain which indicates that the temperature softening effect is greater than strain hardening. As for the ductile properties, the composite exhibits better ductility with the increasing temperature, which means elongation is positively correlated with temperature.

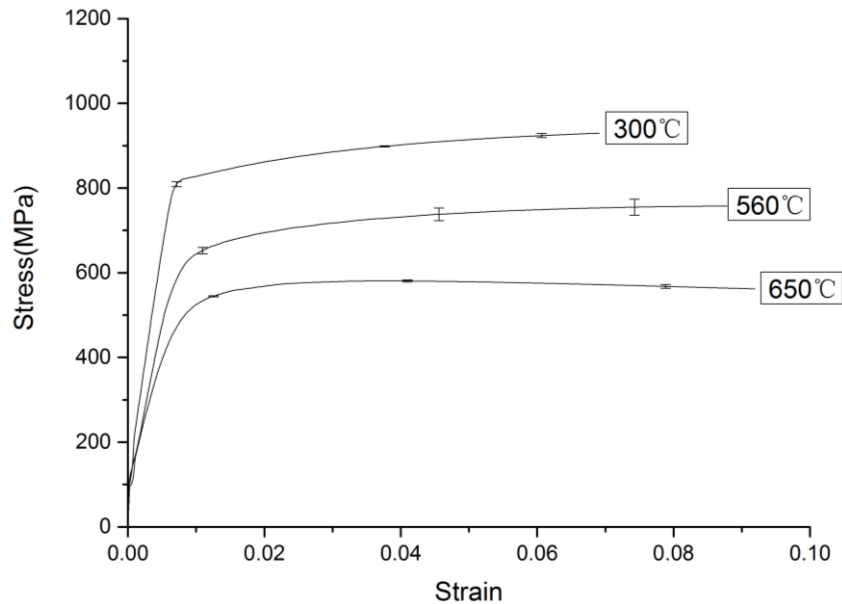


**Figure 3.** Stress-strain curves for the TiC/TMCs composites under quasi-static tensile at different temperatures.

### 3. Meso-Mechanical Theory for Multiphase Composite

#### 3.1. Average Stress of the Reinforcement and the Matrix

Let us consider an  $n$ -phase composite, and we shall refer to the matrix as phase 0, the particle as phase 1, and damaged particle (void) as phase 2. Based on Mori-Tanaka theory, a uniform far-field stress  $\sigma$  is exerted on the composite and its boundary. Take the matrix as comparative material and then the average strain  $\varepsilon^0$  of the comparative material will satisfy Equation (1) under the same external force:

$$\sigma = L_0 : (\varepsilon^0 - \varepsilon_0^p) \quad (1)$$

where  $L_0$  and  $\varepsilon_0^p$  are the stiffness tensor the plastic strain of the matrix, respectively.

Due to the existence of the reinforcement, the average strain is actually different from  $\varepsilon^0$  and perturbation stress  $\tilde{\sigma}$  and perturbation strain  $\tilde{\varepsilon}$  are generated by the interaction between the reinforcement, so the average stress of the matrix is:

$$\sigma^{(0)} = \sigma + \tilde{\sigma} = L_0 : (\varepsilon^0 + \tilde{\varepsilon} - \varepsilon_0^p) \quad (2)$$

Since the elastic property and the coefficient of thermal expansion of the reinforcement is different from that of the matrix, the average stress of the reinforcement is expressed as:

$$\begin{aligned} \sigma^{(1)} = \sigma + \tilde{\sigma} + \sigma_1^{pt} &= L_1 : (\varepsilon^0 + \tilde{\varepsilon} + \varepsilon_1^{pt} - \varepsilon_1^p - \alpha_1^*) \\ &= L_0 : (L_0^{-1} : \sigma + \tilde{\varepsilon} + \varepsilon_1^{pt} - \Delta\varepsilon_1^p - \alpha_1^* - \varepsilon_1^*) \end{aligned} \quad (3)$$

$$\begin{aligned}\sigma^{(2)} = \sigma + \tilde{\sigma} + \sigma_2^{pt} &= L_2 : \left( \varepsilon^0 + \tilde{\varepsilon} + \varepsilon_2^{pt} - \varepsilon_2^p - \alpha_2^* \right) = 0 \\ &= L_0 : \left( L_0^{-1} : \sigma + \tilde{\varepsilon} + \varepsilon_2^{pt} - \Delta\varepsilon_2^p - \alpha_2^* - \varepsilon_2^* \right)\end{aligned}\quad (4)$$

where,  $\sigma_r^{pt}$  and  $\varepsilon_r^{pt}$  indicate the average stress difference and the average strain difference between the  $r$ th phase and the matrix,  $\varepsilon_r^*$  is the eigenstrain of the  $r$ th phase,  $\alpha_r^*$  is caused by the different coefficient of thermal expansion between the  $r$ th phase and the matrix:

$$\alpha_{ij}^{r*} = (\alpha^r - \alpha^0)\Delta T\delta_{ij} = \alpha^r\delta_{ij} \quad (5)$$

$$\varepsilon_r^{pt} = S : \left( \varepsilon_r^* + \Delta\varepsilon_r^p + \alpha_r^* \right) \quad r = 1, 2 \quad (6)$$

where  $\alpha^r$  is the thermal expansion coefficient of the  $r$ th phase.

By using Equations (2), (3), (6), we have:

$$\sigma_r^{pt} = L_0 : (S - I) : \left( \varepsilon_r^* + \Delta\varepsilon_r^p + \alpha_r^* \right) \quad r = 1, 2 \quad (7)$$

where  $S$  is the Eshelby tensor and  $I$  is the four order unit tensor.

The average stress of the composite meets the volume mixing ratio, namely:

$$\sigma = f_0\sigma^{(0)} + f_p\sigma^{(1)} + f_v\sigma^{(2)} \quad (8)$$

where  $f_0 + f_p + f_v = 1$ .

Substitute Equations (2) and (3) into Equation (8), we have:

$$\tilde{\sigma} = -\left( f_p\sigma_1^{pt} + f_v\sigma_2^{pt} \right) \quad (9)$$

and:

$$\tilde{\varepsilon} = (I - S)[f_p(\varepsilon_1^* + \Delta\varepsilon_1^p + \alpha_1^*) + f_v(\varepsilon_2^* + \Delta\varepsilon_2^p + \alpha_2^*)] \quad (10)$$

Let  $X = \varepsilon_1^* + \Delta\varepsilon_1^p + \alpha_1^*$ ,  $Y = \varepsilon_2^* + \Delta\varepsilon_2^p + \alpha_2^*$  and substitute Equation (10) into Equation (4), we get:

$$Y = \frac{f_p X + (I - S)^{-1} L_0^{-1} \sigma}{1 - f_v} \quad (11)$$

Substituting Equation (10) into Equation (3), we have:

$$\begin{aligned}X &= \left\{ L_0 + (L_1 - L_0) : \left[ S - \frac{f_p}{1-f_v}(S - I) \right] \right\}^{-1} : \left[ \frac{1}{1-f_v}(L_0 - L_1) : L_0^{-1} : \sigma + L_1 : (\Delta\varepsilon_1^p + \alpha_1^*) \right] \\ &= \left\{ (1 - f_v - f_p)[(L_1 - L_0) : S + L_0] + f_p L_1 \right\}^{-1} : \left[ (L_0 - L_1) : L_0^{-1} : \sigma + (1 - f_v)L_1 : (\Delta\varepsilon_1^p + \alpha_1^*) \right]\end{aligned}\quad (12)$$

and:

$$\varepsilon_1^* = \left\{ (1 - f_v - f_p)[(L_1 - L_0) : S + L_0] + f_p L_1 \right\}^{-1} : \left[ (L_0 - L_1) : L_0^{-1} : \sigma + (1 - f_v - f_p)(L_0 - L_1) : (S - I) : (\Delta\varepsilon_1^p + \alpha_1^*) \right] \quad (13)$$

$$Y = \left\{ (1 - f_v - f_p)[(L_1 - L_0) : S + L_0] + f_p L_1 \right\}^{-1} : \left\{ [(L_1 - L_0) : S + L_0] : (I - S)^{-1} : L_0^{-1} : \sigma + f_p L_1 : (\Delta\varepsilon_1^p + \alpha_1^*) \right\} \quad (14)$$

$$\begin{aligned}\varepsilon_2^* &= \left\{ (1 - f_v - f_p)[(L_1 - L_0) : S + L_0] + f_p L_1 \right\}^{-1} : \left\{ [(L_1 - L_0) : S + L_0] : (I - S)^{-1} : L_0^{-1} : \sigma + f_p L_1 : (\Delta\varepsilon_1^p + \alpha_1^*) \right. \\ &\quad \left. - [(1 - f_v - f_p)[(L_1 - L_0) : S + L_0] + f_p L_1] : (\Delta\varepsilon_2^p + \alpha_2^*) \right\}\end{aligned}\quad (15)$$

Substituting Equations (1), (10)–(12) into Equations (2) and (3), respectively, we get:

$$\begin{aligned}\sigma^{(0)} = \sigma + L_0 : (I - S) : (f_p X + f_v Y) &= \frac{1}{1-f_v}\sigma + \frac{f_p}{1-f_v}L_0 : (I - S) \\ &: \left\{ (1 - f_v - f_p)[(L_1 - L_0) : S + L_0] + f_p L_1 \right\}^{-1} : \left[ (L_0 - L_1) : L_0^{-1} : \sigma + (1 - f_v)L_1 : (\Delta\varepsilon_1^p + \alpha_1^*) \right]\end{aligned}\quad (16)$$

$$\begin{aligned} \sigma^{(1)} &= \sigma + L_0 : (I - S) : (-(1 - f_p)X + f_v Y) = \frac{1}{1 - f_v} \sigma - \frac{1 - f_v - f_p}{1 - f_v} L_0 : (I - S) \\ &: \{(1 - f_v - f_p)[(L_1 - L_0) : S + L_0] + f_p L_1\}^{-1} : [(L_0 - L_1) : L_0^{-1} : \sigma + (1 - f_v)L_1 : (\Delta \varepsilon_1^p + \alpha_1^*)] \end{aligned} \quad (17)$$

### 3.2. Effective Stiffness Tensor of the Composite

The stress-strain relationship can be written as:

$$\varepsilon = L^{-1} : \sigma \quad (18)$$

The average strain of the composite is the sum of the strain:

$$\varepsilon = f_0 \varepsilon^{(0)} + f_p \varepsilon^{(1)} + f_v \varepsilon^{(2)}$$

Substitute  $\varepsilon^{(0)} = \varepsilon^0 + \tilde{\varepsilon} - \varepsilon_0^p$ ,  $\varepsilon^{(1)} = \varepsilon^0 + \tilde{\varepsilon} + \varepsilon_1^{pt} - \varepsilon_1^p - \alpha_1^*$  and  $\varepsilon^{(2)} = \varepsilon^0 + \tilde{\varepsilon} + \varepsilon_2^{pt} - \varepsilon_2^p - \alpha_2^*$  into Equations (18), (6), (10), we have:

$$\varepsilon = L_0^{-1} : \sigma + f_p \varepsilon_1^* + f_v \varepsilon_2^* \quad (19)$$

Substituting Equations (13) and (15) into Equation (19), we get:

$$\begin{aligned} \varepsilon &= L_0^{-1} : \sigma + f_p \varepsilon_1^* + f_v \varepsilon_2^* = L_0^{-1} : \sigma + f_p \{(1 - f_v - f_p)[(L_1 - L_0) : S + L_0] \\ &+ f_p L_1\}^{-1} : [(L_0 - L_1) : L_0^{-1} : \sigma + (1 - f_v - f_p)(L_0 - L_1) : (S - I) : \\ &(\Delta \varepsilon_1^p + \alpha_1^*)] + f_v \{(1 - f_v - f_p)[(L_1 - L_0) : S + L_0] + f_p L_1\}^{-1} : \\ &\{[(L_1 - L_0) : S + L_0] : (I - S)^{-1} : L_0^{-1} : \sigma + f_p L_1 : (\Delta \varepsilon_1^p + \alpha_1^*) \\ &- \{(1 - f_v - f_p)[(L_1 - L_0) : S + L_0] + f_p L_1\} : (\Delta \varepsilon_2^p + \alpha_2^*)\} \end{aligned} \quad (20)$$

The stiffness tensor of the composite at high temperatures can be derived from Equation (20):

$$\begin{aligned} L^{-1} &= L_0^{-1} + f_p \{(1 - f_v - f_p)[(L_1 - L_0) : S + L_0] + f_p L_1\}^{-1} : [(L_0 - L_1) : L_0^{-1} \\ &+ (1 - f_v - f_p)(L_0 - L_1) : (S - I) : \alpha_1^* : \sigma^{-1}] + f_v \{(1 - f_v - f_p)[(L_1 - L_0) : S \\ &+ L_0] + f_p L_1\}^{-1} : \{[(L_1 - L_0) : S + L_0] : (I - S)^{-1} : L_0^{-1} + f_p L_1 : (\Delta \varepsilon_1^p + \alpha_1^*) : \sigma^{-1}\} \\ &= L_0^{-1} + \{(1 - f_v - f_p)[(L_1 - L_0) : S + L_0] + f_p L_1\}^{-1} \{f_p [(L_0 - L_1) : L_0^{-1} \\ &+ (1 - f_v - f_p)(L_0 - L_1) : (S - I) : \alpha_1^* : \sigma^{-1}] + f_v \{[(L_1 - L_0) : S + L_0] : \\ &(I - S)^{-1} : L_0^{-1} + f_p L_1 : \alpha_1^* : \sigma^{-1}\}\} \end{aligned} \quad (21)$$

## 4. Elastoplastic Analysis of the Composite

### 4.1. Constitutive Model of the Matrix

The elastoplastic relationship of the matrix can be described by modified Ludwik equation:

$$\sigma^{(0)} = \sigma_s^{(0)} + h(\varepsilon_0^p)^n \quad (22)$$

where,  $\sigma_s^{(0)}$  is the yield stress of the matrix;  $h$  and  $n$  are material parameters determined by uniaxial tensile test.

Under monotonic loading, the secant modulus  $E_0^s$  of the matrix is expressed as:

$$E_0^s = \frac{\sigma^{(0)}}{\varepsilon_0^e + \varepsilon_0^p} = \frac{1}{\frac{\sigma_s^{(0)}}{E_0 \sigma^{(0)}} + \frac{\varepsilon_0^p}{\sigma_s^{(0)} + h(\varepsilon_0^p)^n}} \quad (23)$$

where,  $\varepsilon_0^e$  and  $\varepsilon_0^p$  are the elastic strain and the plastic strain of the matrix, respectively.

Under three-dimensional stress, by replacing  $\sigma^{(0)}$  and  $\varepsilon_0^p$  with Mises effective stress  $\sigma^{(0)*}$  and effective strain  $\varepsilon_0^{p*}$ , formula (22) can be rewritten as:

$$\sigma^{(0)*} = \sigma_s^{(0)} + h(\varepsilon_0^{p*})^n \quad (24)$$

where:

$$\sigma^{(0)*} = \left(\frac{3}{2}\sigma_{ij}^{(0)'}\sigma_{ij}^{(0)'}\right)^{\frac{1}{2}}, \varepsilon_0^{p*} = \left(\frac{2}{3}\varepsilon_{ij}^{p(0)}\varepsilon_{ij}^{p(0)}\right)^{\frac{1}{2}} \quad (25)$$

$\sigma_{ij}^{(0)'}$  is the stress deviator of the matrix.

The secant bulk modulus and shear modulus of the matrix are expressed as:

$$k_0^s = \frac{E_0^s}{3(1-2\nu_0^s)}, \quad \mu_0^s = \frac{E_0^s}{2(1+\nu_0^s)} \quad (26)$$

where  $\nu_0^s$  indicates the secant Poisson's ratio.

Due to plasticity incompressibility, the secant bulk modulus  $k_0^s$  is equal to the elastic bulk modulus  $k_0$ , so, we have:

$$\nu_0^s = \frac{1}{2} - \frac{E_0^s}{E_0} \left(\frac{1}{2} - \nu_0\right) \quad (27)$$

In general, the elastoplastic behavior of the matrix under monotonic loading can be described by the secant Young's modulus  $E_0^s$  and two elastic constants  $E_0$  and  $\nu_0$ .

#### 4.2. Stress for the Reinforcement and the Matrix and the Secant Tensor of the Composite under Force Boundary Conditions

When the matrix is in the elastoplastic stage, the modulus changes with the deformation, so the modulus of the matrix takes the secant value indicating by superscript *S*. According to Equations (16) and (17), the stress for the matrix and the reinforcement can be written as:

$$\sigma^{(0)} = \frac{1}{1-f_v}\sigma + \frac{f_p}{1-f_v}L_0^s : (I - S) : \left\{ (1 - f_v - f_p) \right. \\ \left. [(L_1 - L_0^s) : S + L_0^s] + f_p L_1 \right\}^{-1} : \left[ (L_0^s - L_1) : L_0^{s-1} : \sigma + (1 - f_v)L_1 : (\Delta\varepsilon_1^p + \alpha_1^*) \right] \quad (28)$$

$$\sigma^{(1)} = \frac{1}{1-f_v}\sigma - \frac{1-f_v-f_p}{1-f_v}L_0^s : (I - S) : \left\{ (1 - f_v - f_p) \right. \\ \left. [(L_1 - L_0^s) : S + L_0^s] + f_p L_1 \right\}^{-1} : \left[ (L_0^s - L_1) : L_0^{s-1} : \sigma + (1 - f_v)L_1 : (\Delta\varepsilon_1^p + \alpha_1^*) \right] \quad (29)$$

According to Equation (21), the secant tensor of the composite is given:

$$(L^s)^{-1} = (L_0^s)^{-1} + \left\{ (1 - f_v - f_p) [(L_1 - L_0^s) : S + L_0^s] + f_p L_1 \right\}^{-1} \{ f_p [(L_0^s - L_1) \\ : (L_0^s)^{-1} + (1 - f_v - f_p)(L_0^s - L_1) : (S - I) : \alpha_1^*] + f_v \{ [(L_1 - L_0^s) : S + L_0^s] \\ : (I - S)^{-1} : (L_0^s)^{-1} + f_p L_1 : \alpha_1^* \} \} \quad (30)$$

where:

$$L_0^s = (2k_0^s, k_0^s - \mu_0^s, k_0^s - \mu_0^s, k_0^s + \mu_0^s, 2\mu_0^s, 2\mu_0^s) \quad (31)$$

$$L_1 = (2k_1, k_1 - \mu_1, k_1 - \mu_1, k_1 + \mu_1, 2\mu_1, 2\mu_1) \quad (32)$$

$$L_2 = (0, 0, 0, 0, 0, 0) \quad (33)$$

$$I = (1, 0, 0, 1, 1, 1) \quad (34)$$

$$S = \left( \frac{2}{3}\alpha^s, \frac{\alpha^s}{3} - \frac{\beta^s}{2}, \frac{\alpha^s}{3} - \frac{\beta^s}{2}, \frac{\alpha^s}{3} + \frac{\beta^s}{2}, \beta^s, \beta^s \right) \quad (35)$$

$$\alpha^s = \frac{1 + v_0^s}{3(1 - v_0^s)}, \quad \beta^s = \frac{2(4 - 5v_0^s)}{15(1 - v_0^s)} \quad (36)$$

#### 4.3. Interfacial Debonding Model

In order to describe the propagation of the interfaces, Weibull statistical distribution is introduced to discuss the cumulative probability of the interfacial debonding.

It is assumed that when the interfacial debonding happened between the matrix and the reinforcement (particle), the particle cannot bear any load and can be equivalent to a hole. By assuming that the tensile stress in the particle controls the debonding and the initial propagation strength along  $ii$  direction meets the Weibull statistical distribution  $P_{ii}$  [35], we have:

$$P_{ii}(\sigma_{11}^{(1)}) = 1 - \exp\left[-\left(\frac{\sigma_{ii}^{(1)}}{s}\right)^m\right], \quad i = 1, 2, 3 \quad (37)$$

where,  $P_{ii}(\sigma_{11}^{(1)})$  is the ratio of the damaged particles to all particles, i.e., the debonding probability.  $s$  and  $m$  are scale parameter and shape parameter of the Weibull function. Thus, the volume fraction of the damaged particle on the composite is:

$$f_1 P_{11}(\sigma_{11}^{(1)}) = f_1 \left\{ 1 - \exp\left[-\left(\frac{\sigma_{11}^{(1)}}{s}\right)^m\right] \right\} \quad (38)$$

The probability density of the damaged interface can be written as:

$$p_{11}(\sigma_{11}^{(1)}) = \frac{m}{s} \exp\left(\frac{\sigma_{11}^{(1)}}{s}\right)^{m-1} \left[-\left(\frac{\sigma_{11}^{(1)}}{s}\right)\right]^m \quad (39)$$

The relationship between the critical debonding strength of the interface  $\sigma_c$  and the two parameters  $s$  and  $m$  is given as [36]:

$$\sigma_c = \int_0^\infty \sigma_{11}^{(1)} p d\sigma_{11}^{(1)} = s \cdot \Gamma\left(1 + \frac{1}{m}\right) \quad (40)$$

When the critical debonding strength of the interface  $\sigma_c$  and the loading exerted on the particle are known, the volume fraction of the debonding particle can be obtained by Equation (37).

#### 4.4. Elastoplastic Stress-Strain Relationship

The damage constitutive relation can be expressed by Equation (30). When the matrix is in the plastic stage,  $L_0^s$  is not a constant and changes with the deformation process. At the same time, volume fraction  $f_p$  and  $f_v$  are also changing. So, in order to obtain the stress-strain relationship,  $L_0^s$  and  $f_v$  of each stage should be calculated firstly. The numerical calculation is performed according to the following procedure: (1) calculate the effective elastic modulus  $L$  of the material and taking as the initial value; (2) for a given  $\sigma$ , determining  $\sigma^{(0)}$  and  $\sigma^{(1)}$  from Equations (28) and (29); (3) set  $\sigma_c$  and  $m$ , deriving  $f_v$  from Equation (37) ( $f_p = f_1 - f_v$ ) and then obtaining the effective stress of the matrix from  $\sigma^{(0)}$ . If  $\sigma^{(0)}$  is bigger than the elastic limit  $\sigma_s^{(0)}$  of the matrix,  $L_s^0$  should be calculated from Equations (23), (26), (27), (31); and (4) increasing  $\sigma$  and calculating  $L^s$  from the new  $L_s^0$ , then repeating the whole process.

It is assumed that the elastic modulus of the TiC particle does not change with the changes in temperature and the elastic modulus of the matrix decreases with the increase of temperature. In order to obtain the elastic of the matrix at different temperature, we assume that the elastic modulus of the matrix decreases linearly with increasing temperature. Based the known elastic modulus of the matrix, the elastic modulus at different temperatures can be obtained. The elastic modulus and yield

stress of the matrix at room temperature was experimentally determined. By assuming that there are linear relationships between elastic modulus and temperature, and yield stress with temperature, respectively, the elastic modulus and yield stress of the matrix at different temperatures was calculated, which was shown in Table 1.

**Table 1.** The elastic modulus and yield stress of the matrix at different temperatures.

Temperature	R.T.	300 °C	600 °C	650 °C	700 °C
$E_0$ /GPa	113	71	25	20	15
$\sigma_s^{(0)}$ /MPa	1050	670	590	540	420

## 5. Comparison of Numerical Predictions with Experimental Results

When the uniaxial tensile stress  $\sigma_{11}$  is exerted on the particle-reinforced titanium matrix composite at high temperatures, the material parameters of the composite is listed as follows:  $\nu_0 = 0.35$ ,  $E_1 = 460$  Gpa,  $\nu_1 = 0.188$ ,  $f_1 = 0.03$ ,  $h = 60$  Mpa,  $n = 0.45$ ,  $\sigma_c = 2.0\sigma_s^{(0)}$ ,  $m = 5$ . The stress-strain curves of the composite at three different temperatures ( $T = 300$  °C,  $560$  °C,  $650$  °C) are shown in Figure 4.

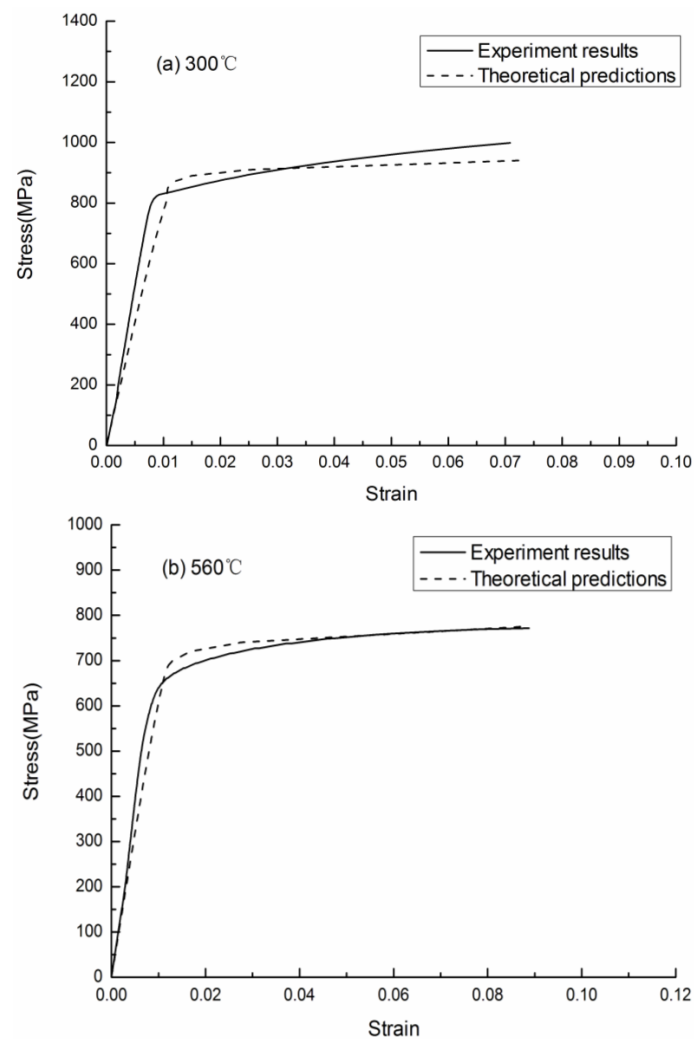


**Figure 4.** Cont.

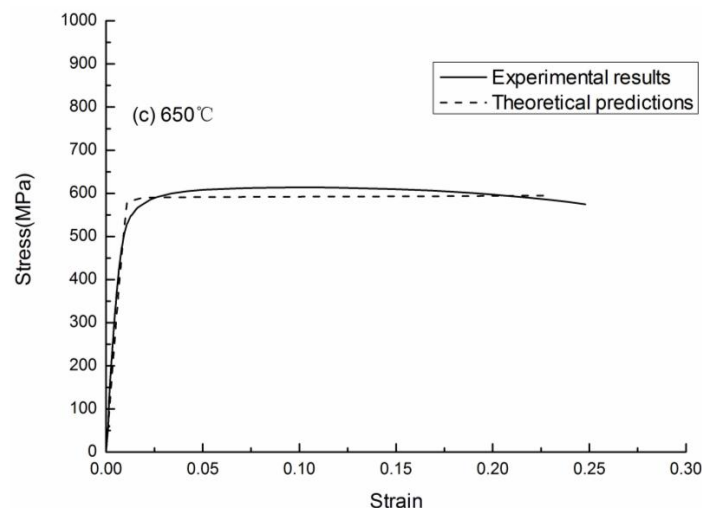


**Figure 4.** Comparisons of stress-strain curves of TiC/TMCs composites with the theoretical results and test results at different temperatures: (a) 300 °C; (b) 560 °C; and (c) 650 °C.

From Figure 4, it can be seen that the numerical predictions agree well with experimental results, which demonstrate the assumption that the elastic modulus decreases linearly with the increase of the temperature. The debonding model adopted in the current paper can be used to predict the elastoplastic behavior of the composite at elevated temperatures. There is little discrepancy of initial elastic modulus and yield stress, which may be caused by that the theoretical model did not consider the particle cracking and ductile fracture. Nevertheless, in the plastic section of the curve, the theoretical model prediction is not accurate enough, which needs further study.

## 6. Conclusions

Based on Eshelby's theory and Mori-Tanaka theory, the stress of the reinforcement and the matrix and the effective stiffness tensor of the composite under force boundary conditions are deduced. By using the assumption that the interfacial debonding is controlled by the tensile stress on the particle and the cumulative probability of the interfacial debonding is described by the Weibull function, a meso-mechanical constitutive model is proposed to investigate the elastoplastic properties of the particle-reinforced titanium matrix composite by using the secant modulus method. A good agreement between the numerical predictions and the experimental results is obtained, which demonstrate that the model and the method adopted in the current study is reliable and reasonable. When particle-reinforced titanium matrix composites were used at high temperatures, such as in aerospace and automobile industries, this model can be used to predict the mechanical properties so as to provide the theoretic basis for the design of structural parameters.

**Acknowledgments:** The author acknowledges the financial support of the National Nature Science Foundation of China (11672043, 11521062, 11325209), the Opening Project of State Key Laboratory for Strength and Vibration of Mechanical Structures (SV2015-KF-10), the Opening Project of State Key Laboratory of Traction Power (TPL1701) and the Project of State Key Laboratory of Explosion Science and Technology (YBKT16-19, KFJJ15-02M).

**Author Contributions:** Weidong Song conceived and designed the study; Liansong Dai and Lijun Xiao performed the experiments and analyzed the data; Weidong Song, Liansong Dai, Lijun Xiao and Cheng Wang made the theoretical analysis; Xiaonan Mao and Huiping Tang provided the specimens and essential parameters of the material; Weidong Song and Liansong Dai wrote the paper. All authors read and approved the manuscript.

**Conflicts of Interest:** The authors declare no conflict of interest.

## References

1. Hunt, M. MMCs for exotic needs. *Compos. Mater. Sci.* **1992**, *104*, 53–62.
2. Gorynin, I.V. Titanium alloys for marine application. *Mater. Sci. Eng. A* **1999**, *263*, 112–116. [[CrossRef](#)]

3. Schutz, R.W.; Scaturro, M.R. An overview of current and candidate titanium alloy applications on U.S. navy surface ships. *Nav. Eng. J.* **1991**, *175–191*. [[CrossRef](#)]
4. Luo, Y.Z. Recent development of titanium metallic matrix composites. *Rare Met. Mater. Eng.* **1997**, *26*, 1–7.
5. Vallauri, D.; Adrian, I.C.A.; Chrysanthou, A. TiC-TiB<sub>2</sub> composites: A review of phase relationships, processing and properties. *J. Eur. Ceram. Soc.* **2008**, *28*, 1697–1713. [[CrossRef](#)]
6. Leyens, C.; Peters, M. *Titanium and Titanium Alloys*; Wiley-VCH: Cologne, Germany, 2003.
7. Tjong, S.C.; Ma, Z.Y. Microstructural and mechanical characteristics of in-situ metal matrix composites. *Mater. Sci. Eng. R* **2000**, *29*, 49–113. [[CrossRef](#)]
8. Tjong, S.C.; Mai, Y.W. Processing-structure-property aspects of particulate- and whisker-reinforced titanium matrix composites. *Compos. Sci. Technol.* **2008**, *68*, 583–660. [[CrossRef](#)]
9. Wang, X.H.; Zou, Z.D.; Qu, S.Y.; Song, S.L. Microstructure and wear properties of Fe-based hardfacing coating reinforced by TiC particles. *J. Mater. Process. Technol.* **2005**, *168*, 89–94. [[CrossRef](#)]
10. Akhtar, F.; Guo, S.J. Microstructure, mechanical and fretting wear properties of TiC-stainless steel composites. *Mater. Charact.* **2008**, *59*, 84–90. [[CrossRef](#)]
11. Gu, D.D.; Hagedorn, Y.C.; Meiners, W.; Wissenbach, K.; Poprawe, R. Nanocrystalline TiC reinforced Ti matrix bulk-form nanocomposites by Selective Laser Melting (SLM): Densification, growth mechanism and wear behavior. *Compos. Sci. Technol.* **2011**, *71*, 1612–1620. [[CrossRef](#)]
12. Gu, D.D.; Meng, G.B.; Li, C.; Meiners, W.; Poprawe, R. Selective laser melting of TiC/Ti bulk nanocomposites: Influence of nanoscale reinforcement. *Scr. Mater.* **2012**, *67*, 185–188. [[CrossRef](#)]
13. Tohgo, K.; Weng, G.J. A Progressive Damage Mechanics in Particle-reinforced Metal-Matrix Composites under High Triaxial Tension, *Trans. of ASME. J. Eng. Mater. Technol.* **1994**, *116*, 414–420. [[CrossRef](#)]
14. Tohgo, K.; Chou, T.W. Incremental Theory of Particulate-Reinforced Composites Including Debonding Damage. *JSME Int. J. Ser. A* **1996**, *39*, 389–397. [[CrossRef](#)]
15. Tohgo, K.; Itoh, Y.; Shimamura, Y. A Constitutive Model of Particulate-Reinforced Composites Taking Account of Particle Size Effects and Damage Evolution. *Compos. A* **2010**, *41*, 313–321. [[CrossRef](#)]
16. Tohgo, K.; Fujii, T.; Shimamura, D.K.Y. Influence of Particle Size and Debonding Damage on an Elastic-Plastic Singular Field around a Crack-Tip in Particulate-Reinforced Composites. *Acta Mech.* **2014**, *225*, 1373–1389. [[CrossRef](#)]
17. Li, W.; Song, W.D.; Ning, J.G.; Mao, X.N. Effects of strain rate and temperature on mechanical properties of TP-650 composite. *Rare Mater. Eng.* **2010**, *39*, 1195–1199.
18. Song, W.D.; Ning, J.G.; Mao, X.N.; Tang, H.P. A modified Johnson-Cook model for titanium matrix composites reinforced with titanium carbide particles at elevated temperatures. *Mater. Sci. Eng. A* **2013**, *576*, 280–289. [[CrossRef](#)]
19. Eshelby, J.D. The determination of the elastic field of an ellipsoidal inclusion and related problems. *Proc. R. Soc. Lond.* **1957**, *241A*, 376–396. [[CrossRef](#)]
20. Eshelby, J.D. The elastic field outside an ellipsoidal inclusion. *Proc. R. Soc. Lond.* **1959**, *252A*, 561–569. [[CrossRef](#)]
21. Hill, R. A self-consistent mechanics of composite materials. *J. Mech. Phys. Solids* **1965**, *13*, 213–222. [[CrossRef](#)]
22. Budiansky, B. On the elastic model of some heterogeneous materials. *J. Mech. Phys. Solids* **1976**, *12*, 81–97.
23. Morit, T.; Tanaka, K. Average stress in matrix and average energy of materials with misfitting inclusions. *Acta Metall.* **1973**, *21*, 571–574. [[CrossRef](#)]
24. Roscoe, R.A. The Viscosity of suspensions of rigid spheres. *Br. J. Appl. Phys.* **1952**, *3*, 267–269. [[CrossRef](#)]
25. Hashin, Z.; Shtrikman, S. A variational approach to the theory of the elastic behaviour of multiphase materials. *J. Mech. Phys. Solids* **1963**, *11*, 127–140. [[CrossRef](#)]
26. Hashin, Z.; Shtrikman, S. A variational approach to the theory of the effective magnetic permeability of multi-phase materials. *J. Mech. Phys. Solids* **1962**, *10*, 335–342. [[CrossRef](#)]
27. Buryachenko, V. Elastic-plastic behavior of elastically homogeneous materials with a random field of inclusions. *Int. J. Plast.* **1999**, *15*, 687–720. [[CrossRef](#)]
28. Hu, G.K. Composite plasticity based on matrix average second order stress moment. *Int. J. Plast.* **1997**, *12*, 1007–1015. [[CrossRef](#)]
29. Tandon, P.; Weng, G.J. A theory of particle-reinforced plasticity. *ASME J. Appl. Mech.* **1991**, *55*, 126–135. [[CrossRef](#)]

30. Song, W.; Yang, Y.; Ning, J. A Meso-Mechanical Constitutive Model of Particle Reinforced Titanium Matrix Composites Subjected to Impact Loading. *J. Nano Res.* **2013**, *23*, 104–107. [[CrossRef](#)]
31. Lissenden, C.J. Fiber-matrix interfacial constitutive relations for metal matrix composites. *Compos. B* **1999**, *30*, 267–278. [[CrossRef](#)]
32. Lee, H.K.; Pyo, S.H. An elastoplastic multi-level damage model for ductile matrix composites considering evolutionary weakened interface. *Int. J. Solid Struct.* **2008**, *45*, 1614–1631. [[CrossRef](#)]
33. Xia, S.H.; Wang, J.T. A micromechanical model of toughening behavior in the dual-phase composite. *Int. J. Plast.* **2010**, *26*, 1442–1460. [[CrossRef](#)]
34. Song, W.D.; Ning, J.G.; Wang, J. Mechanical Behavior of Titanium Carbide Particle-Reinforced Titanium Matrix Composite under Quasi-Static and Dynamic Tension. *Adi. Sci. Lett.* **2011**, *4*, 635–640. [[CrossRef](#)]
35. Weibull, W. A statistical distribution function of side applicability. *J. Appl. Mech.* **1951**, *18*, 293–297.
36. Zhao, Y.H.; Weng, G.J. Plasticity of a two-phase composite with partially debonded inclusions. *Int. J. Plast.* **1996**, *12*, 781–804. [[CrossRef](#)]



© 2017 by the authors; licensee MDPI, Basel, Switzerland. This article is an open access article distributed under the terms and conditions of the Creative Commons Attribution (CC-BY) license (<http://creativecommons.org/licenses/by/4.0/>).